

Triazole derivatives as non-nucleoside inhibitors of HIV-1 reverse transcriptase—Structure–activity relationships and crystallographic analysis

Thorsten A. Kirschberg,* Mini Balakrishnan, Wei Huang, Rebecca Hluhanich, Nilima Kutty, Albert C. Licican, Damian J. McColl, Neil H. Squires and Eric B. Lansdon

Gilead Sciences, Department of Medicinal Chemistry, 333 Lakeside Drive, Foster City, CA 94404, USA

Received 19 October 2007; revised 27 November 2007; accepted 30 November 2007
Available online 5 December 2007

Abstract—A series of 3,4,5-trisubstituted 1,2,4-*H* triazole derivatives was synthesized and investigated for HIV-1 reverse transcriptase inhibition. An X-ray structure with HIV-1 RT secured the binding mode and allowed the key interactions with the enzyme to be identified.

© 2007 Elsevier Ltd. All rights reserved.

Despite their longstanding use in the context of highly active anti-retroviral therapy (HAART) for the treatment of HIV infections, non-nucleoside reverse-transcriptase inhibitors (NNRTIs) continue to be the focus of much pharmaceutical research.¹ Three NNRTIs are currently approved for clinical use: Efavirenz, Nevirapine, and Delavirdine (Fig. 1). Other compounds, such as TMC-125 and TMC-278, have entered late stage clinical trials.² Mode of action studies for this class reveal evidence for multiple binding modes in the target pocket within HIV-1 RT, suggestive of a role in raising the barrier to drug resistance development.³ Further detailed investigations have revealed hitherto undescribed inhibitory modes of action for this structurally diverse class of compounds, most notably the pronounced inhibition of viral DNA plus strand synthesis from RNA primers and effects on the RNase H function of HIV-RT⁴.

Recently, different groups have disclosed efforts using triazole or tetrazole derived scaffolds as templates for the design and synthesis of novel inhibitors of HIV-1 RT.⁵ Representative structures are depicted in Figure 2. In these studies, much emphasis was placed on control of key NNRTI-resistant mutants of HIV-1 RT: K103N, Y181C, Y188C, alone or in combination. Compound 4

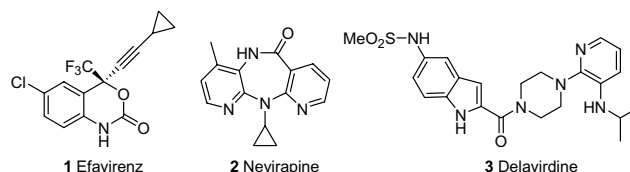


Figure 1. Structures of FDA-approved NNRTIs.

represents the clinical candidate VRX-480773 with good overall resistance profile in vitro.

While structures 4 and 5 are derived from relatively large compound collections of structurally related entities, only few analogs of 6 have been reported. Due to the modular assembly of this lead, we chose to investigate this rather simple, yet highly flexible starting point further.

The synthesis of the 3,4,5-trisubstituted 1,2,4-*H*-triazoles, based on earlier work in this structural class by Kane et al. in an unrelated therapeutic area, is depicted in Scheme 1.⁶ Generation of the desired compounds was straightforward and was further simplified by their tendency to precipitate from the reaction mixture. In short, hydrazides were formed in two steps from the corresponding acid chloride (defining substituent R¹). These hydrazides were reacted with substituted isothiocyanates (R²) at slightly elevated temperatures. Cyclization of the crude material to the triazole occurred under aqueous

Keywords: HIV-1 reverse transcriptase; NNRTI.

* Corresponding author. Tel.: +1 650 522 5133; fax: +1 650 522 5899; e-mail: tkirschberg@gilead.com

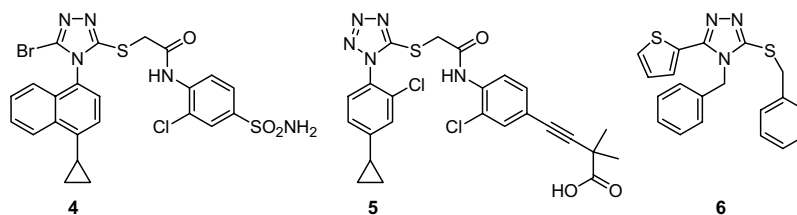
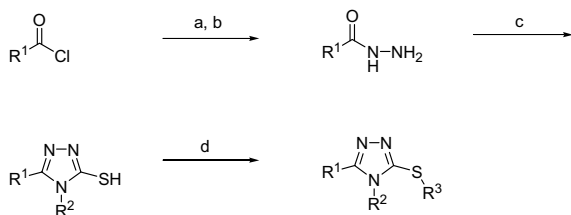


Figure 2. Representative examples of recently disclosed azole-based inhibitors of HIV RT.



Scheme 1. Route employed for the synthesis of substituted triazoles. Reagents and conditions: (a) H_2NNHBoc , TEA, THF, rt; (b) HCl (4 N), dioxane, rt; (c) i: $\text{R}^2\text{-NCS}$, THF, 65 °C; ii: NaHCO_3 aq, 100 °C; (d) $\text{R}^3\text{-Br}$, Cs_2CO_3 , acetonitrile, rt. R^1 , R^2 , and R^3 are used consistently throughout this document including Tables 1–3.

conditions in the presence of mild base. Finally, *S*-alkylation was achieved via reaction with activated alkyl and benzylic bromides in the presence of cesium carbonate in acetonitrile. Products were isolated either via filtration (after water addition to the crude reaction to dissolve all inorganic salts) or following reverse-phase HPLC purification and lyophilization.⁷

Table 1 summarizes the results obtained for seven simple derivatives sharing a 2'-thiophenyl substituent as R^1 and a benzyl group as R^3 . The 4-benzyl derivative (**6**) was the only one that displayed anti-HIV activity, albeit with a moderate selectivity index.⁸ Shortening or lengthening the distance of the phenyl ring from the core or removing it altogether led to dramatic loss of activity, as did the introduction of chlorine or methoxy substituents. Based on these results, further SAR studies were performed with an unmodified benzyl substituent at R^2 .

Table 1. Antiviral effect for compounds 6–12⁹

Compound	R^2	EC_{50}^a (μM)	S.I. ^b
6	CH_2Ph	3.7	8
7	Me	>100	na
8	Ph	>100	na
9	$\text{CH}_2\text{CH}_2\text{Ph}$	>100	na
10	$\text{CH}_2(4'\text{-OMePh})$	>100	na
11	$\text{CH}_2(4'\text{-ClPh})$	>100	na
12	$\text{CH}_2(3'\text{-Cl}, 4'\text{-ClPh})$	>100	na

^a Values are means of at least two independent experiments. The activity was determined in a standard 5-day infectivity assay using MT-4 cell-line and virally induced cell death as the read-out.

^b In vitro selectivity index (EC_{50} cytotoxicity/ EC_{50} antiviral effect).

Structure–activity relationships at R^1 were initially examined with both R^2 and R^3 fixed as unsubstituted benzyl groups and are summarized in Table 2. In general, all changes explored (even conservative ones such as the isosteric thiophene **16**) led to a loss in activity and/or erosion in the selectivity index.

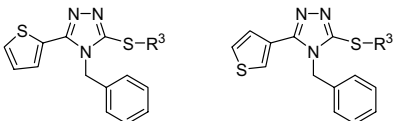
The highest degree of structural diversity was introduced at position 3 of the triazole core. A selected dataset is summarized in Table 3, focusing on thiophenyl substituents as R^1 . The replacement of the aromatic ring with alkyl substituents led to loss of antiviral activity, while extension of the linker by one methylene unit (**22** and **39**) reduced the activity by more than an order of magnitude. The introduction of a pyridine substituent (**23–25** and **40–42**) yielded slightly less active compounds when compared to the parent (**6**). The antiviral activity was relatively insensitive to the exact location of the nitrogen atom. Inspired by the work of Topliss the effects of substituents on the aromatic ring were examined, initially focusing on meta- and para-positions, alone or in combination.¹⁰ While *p*-chloro and methoxy substituents enhanced potency, the introduction of a nitrile led to considerable loss of activity. Focusing on mono-chloro derivatives at different positions, the antiviral activity was improved by more than an order of magnitude (**30** vs **6** and **47** vs **16**) when a chloro substituent was placed in the *ortho* position. Furthermore, while the *ortho*-chloro substitution enhanced the activity, it did not increase the cytotoxicity, resulting in a much improved selectivity index. While structurally distinct, it is interesting to note that a variety of newer

Table 2. Antiviral effect for selected R^1 variants

Compound	R^1	EC_{50}^a (μM)	S.I. ^b
13	Me	23.5	2
14	Ph	10.5	1.1
15	2'-Furanyl	4.6	5.2
16	3'-Thiophenyl	9.2	2
17	$\text{CH}_2(2'\text{-thiophenyl})$	>100	na
18	2'-Benzothiophenyl	>100	na
19	2'-ClPh	2.85	2.9

^a Values are means of at least two independent experiments. The activity was determined in a standard 5-day infectivity assay using MT-4 cell-line and virally induced cell death as the read-out.

^b In vitro selectivity index (EC_{50} cytotoxicity/ EC_{50} antiviral effect).

Table 3. Antiviral effect for compounds **20–53**


Compound	R ¹	R ³	EC ₅₀ ^a (μM)	S.I. ^b
20	2'-Thiophenyl	Me	>100	na
21	2'-Thiophenyl	<i>n</i> -Hexyl	>100	na
22	2'-Thiophenyl	CH ₂ CH ₂ Ph	28.5	≤1
23	2'-Thiophenyl	CH ₂ (2'-pyridyl)	8.3	5
24	2'-Thiophenyl	CH ₂ (3'-pyridyl)	8.3	6
25	2'-Thiophenyl	CH ₂ (4'-pyridyl)	4.8	15
26	2'-Thiophenyl	CH ₂ (4'-CIPh)	2	5.7
27	2'-Thiophenyl	CH ₂ (4'-OMePh)	3	3.8
28	2'-Thiophenyl	CH ₂ (4'-CNPh)	23.5	< 1
29	2'-Thiophenyl	CH ₂ (3'-CIPh)	1.7	5.3
30	2'-Thiophenyl	CH ₂ (2'-CIPh)	0.44	35.2
31	2'-Thiophenyl	CH ₂ (2'-Cl,3'-CIPh)	0.73	9.1
32	2'-Thiophenyl	CH ₂ (2'-Cl,4'-CIPh)	1.1	7.7
33	2'-Thiophenyl	CH ₂ (2'-Cl,5'-CIPh)	1.0	7.9
34	2'-Thiophenyl	CH ₂ (2'-Cl,6'-CIPh)	3.45	1.7
35	2'-Thiophenyl	CH ₂ (3'-Cl,4'-CIPh)	2.4	3.1
36	2'-Thiophenyl	CH ₂ (2'-naphthyl)	1.7	5.9
37	3'-Thiophenyl	Me	>100	na
38	3'-Thiophenyl	<i>n</i> -Hexyl	>100	na
39	3'-Thiophenyl	CH ₂ CH ₂ Ph	>100	na
40	3'-Thiophenyl	CH ₂ (2'-pyridyl)	>100	na
41	3'-Thiophenyl	CH ₂ (3'-pyridyl)	23	2
42	3'-Thiophenyl	CH ₂ (4'-pyridyl)	41.5	1
43	3'-Thiophenyl	CH ₂ (4'-CIPh)	51.1	≤1
44	3'-Thiophenyl	CH ₂ (4'-OMePh)	5.8	1
45	3'-Thiophenyl	CH ₂ (4'-CNPh)	>100	na
46	3'-Thiophenyl	CH ₂ (3'-CIPh)	1.6	6.3
47	3'-Thiophenyl	CH ₂ (2'-CIPh)	0.131	62
48	3'-Thiophenyl	CH ₂ (2'-Cl,3'-CIPh)	1.3	5
49	3'-Thiophenyl	CH ₂ (2'-Cl,4'-CIPh)	3.3	2.9
50	3'-Thiophenyl	CH ₂ (2'-Cl,5'-CIPh)	8.95	1.6
51	3'-Thiophenyl	CH ₂ (2'-Cl,6'-CIPh)	>100	na
52	3'-Thiophenyl	CH ₂ (3'-Cl,4'-CIPh)	4.7	1.2
53	3'-Thiophenyl	CH ₂ (2'-naphthyl)	0.58	11.1

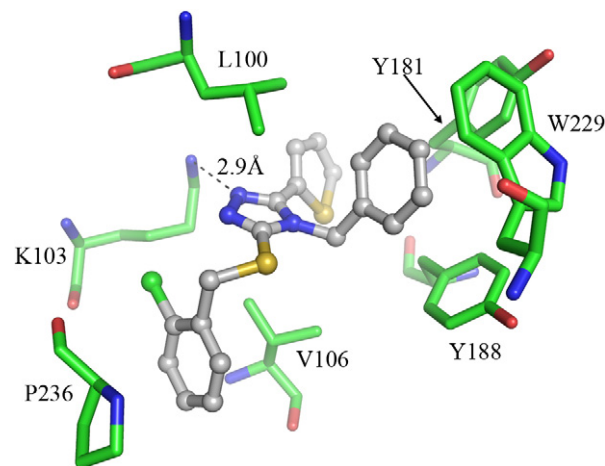
^a Values are means of at least two independent experiments. The activity was determined in a standard 5-day infectivity assay using MT-4 cell-line and virally induced cell death as the read-out.

^b In vitro selectivity index (EC₅₀ cytotoxicity/EC₅₀ antiviral effect).

NNRTIs share a small *ortho* substituent on the terminal ring—for example, **4**, **5** (chloro), and GW-678248 (methyl).¹¹ Compounds **30** and **47** represent the most active NNRTIs in this report. For neither of these did the introduction of a second chlorine on the aromatic ring lead to a benefit; these analogs were clearly inferior with respect to activity and selectivity index.

A crystal of compound **30** bound to HIV-RT was obtained and its structure was determined at a resolution of 2.3 Å by X-ray diffraction.¹² The bound ligand is depicted in Figure 3. Compound **30** is found in the classical NNRTI binding pocket within the p66 subunit of HIV-1 RT.

The structure illuminates the SAR data discussed above. Consistent with the strong preference for a benzylic sub-

**Figure 3.** Structure of compound **30** in complex with HIV-1 RT.

stituent at R², a close interaction with the protein is seen for this region of the ligand, buried in the lipophilic groove formed by the side chains of Tyr181, Tyr188, and Trp229. The benzyl group is forming close contacts with the aromatic side chains of Tyr181 and Tyr188, whereas it forms an edge-on contact to the plane of the indole ring of Trp229. Furthermore, the side-chain amino group of Lys103 is found in close proximity to the nitrogen N1 of the triazole, indicative of the presence of a hydrogen bond. The thiophene group at R¹ is positioned toward the peptide backbone of Ile180 and between the side chains of Val179 and Tyr181. Failure to occupy this lipophilic pocket results in a loss of activity as seen for compound **13**. The *ortho*-chloro benzyl group is positioned between Pro236 and Val106 in a channel leading to solvent. This channel is observed with many NNRTIs. Finally, a *van-der-Waals* interaction of Val106 with the triazole scaffold is seen. This residue plays a key role in resistance development to this class of compounds, typified by studies with the parent analog **6**, for which V106I was the first mutation detected with other more typical NNRTI-induced mutations being generated subsequently.¹³ Presumably the increased steric bulk of the isoleucine side chain provides the basis for this resistance.

In summary, a concise set of 3,4,5-trisubstituted 1,2,4-*H* triazoles was synthesized and evaluated for anti-HIV activity. Binding to the NNRTI binding site was established via X-ray crystallography. Antiviral activity was moderate and compromised in general by a low selectivity index. The introduction of an *ortho*-chloro substituent on the *S*-benzyl group considerably improved the antiviral potency without a concomitant increase in cytotoxicity.

Acknowledgments

The authors thank the high-throughput purification group at Gilead Sciences for the support of this work: Amy Kwok, Mona Cai, and David Cowfer. Additionally, the authors thank William J. Watkins and Jay P. Parrish for helpful discussions.

References and notes

- (a) Boone, L. R. *Curr. Opinion Invest. Drugs* **2006**, 7, 128; (b) Balzarini, J. *Curr. Topics Med. Chem.* **2004**, 4, 921; (c) Zhang, Z.; Hamatake, R.; Hong, Z. *Antiviral Chem. Chemotherapy* **2004**, 15, 121.
- (a) Janssen, P. A.; Lewi, P. J.; Arnold, E.; Daeyaert, F.; Jonge, M.; Heeres, J.; Koymans, L.; Vinkers, M.; Guillemont, J.; Pasquier, E.; Kukla, M.; Ludovici, D.; Andries, K.; Bethune, M.-P.; Pauwels, R.; Das, K.; Clark, A. D.; Frenkel, Y. V.; Hughes, S. H.; Medaer, B.; Knaep, F.; Bohets, H.; Clerck, F.; Lampo, A.; Williams, P.; Stoffels, P. *J. Med. Chem.* **2005**, 48, 1901; (b) Guillemont, J.; Pasquier, E.; Palandjian, P.; Vernier, D.; Gaurrand, S.; Lewi, P. J.; Heeres, J.; Jonge, M. R.; Koymans, L. M. H.; Daeyaert, F. F. D.; Vinkers, M. H.; Arnold, E.; Das, K.; Pauwels, R.; Andries, K.; Bethune, M.-P.; Bettens, E.; Hertogs, K.; Wigerninck, P.; Timmermans, P.; Janssen, P. A. *J. J. Med. Chem.* **2005**, 48, 2072.
- Das, K.; Lewi, P. J.; Hughes, S. H.; Arnold, E. *Prog. Biophys. Mol. Biol.* **2005**, 88, 209.
- (a) Grobler, J. A.; Dornadula, G.; Rice, M. R.; Simcoe, A. L.; Hazuda, D. J.; Miller, M. D. *J. Biol. Chem.* **2007**, 282, 8005; (b) Hang, J. Q.; Li, Y.; Yang, Y.; Cammack, N.; Mirzadegan, T.; Klumpp, K. *Biochem. Biophys. Res. Comm.* **2007**, 352, 341; (c) Shaw-Reid, C. A.; Feuston, B.; Munshi, V.; Getty, K.; Krueger, J.; Hazuda, D. J.; Parniak, M. A.; Miller, M. D.; Lewis, D. *Biochemistry* **2005**, 44, 1595.
- Structure 4 (a) Zhang, Z.; Xu, W.; Koh, Y.-H.; Shim, J. H.; Girardet, J.-L.; Yeh, L.-T.; Hamatake, R. K.; Hong, Z. *Antimicrobial Agents Chemother.* **2007**, 51, 429; (b) De La Rosa, M.; Kim, H. W.; Gunic, E.; Jenket, C.; Boyle, U.; Koh, Y.-H.; Korboukh, I.; Allan, M.; Zhang, W.; Chen, H.; Xu, W.; Nilar, S.; Yao, N.; Hamatake, R.; Lang, S. A.; Hong, Z.; Zhang, Z.; Girardet, J.-L. *Bioorg. Med. Chem. Lett.* **2006**, 16, 4444; Structure 5; (c) Gagnon, A.; Amad, M. H.; Bonneau, P. R.; Coulombe, R.; DeRoy, P. L.; Doyon, L.; Duan, J.; Garneau, M.; Guse, I.; Jakalian, A.; Jolicoeur, E.; Landry, S.; Malenfant, E.; Simoneau, B.; Yoakim, C. *Bioorg. Med. Chem. Lett.* **2007**, 17, 4437; (d) Structure 6: Olsen, M. W.; Di Grandi, M. Appl. 2005 WO 2005/090320 A2; Related work: (e) Wang, Z.; Wu, B.; Kuhen, K. L.; Bursulaya, B.; Nguyen, T. N.; Nguyen, D. G.; He, Y. *Bioorg. Med. Chem. Lett.* **2006**, 16, 4174; (f) Muraglia, E.; Kinzel, O. D.; Laufer, R.; Miller, M. D.; Moyer, G.; Munshi, V.; Orvieto, F.; Palumbi, M. C.; Pescatore, G.; Rowley, M.; Williams, P. D.; Summa, V. *Bioorg. Med. Chem. Lett.* **2006**, 16, 2748.
- (a) Kane, J. M.; Staeger, M. A.; Dalton, C. R.; Miller, F. P.; Dudley, M. W.; Ogden, A. M. L.; Kehne, J. H.; Ketteler, H. J.; McCloskey, T. C.; Senyah, Y.; Chmielewski, P. A.; Miller, J. A. *J. Med. Chem.* **1994**, 37, 125; (b) Kane, J. M.; Baron, B. M.; Dudley, M. W.; Sorensen, S. M.; Staeger, M. A.; Miller, F. P. *J. Med. Chem.* **1990**, 33, 2772.
- All compounds were characterized by ^1H NMR spectroscopy and LC-MS analysis. Purities were assessed via analytical RP-HPLC and are >95%.
- The logD for compound **6** was measured to be 3.5 and we did not anticipate problems with membrane permeability for this class given the body of work cited in Ref. 5.
- Efavirenz (**1**) activity under these conditions (MT-4 cells): EC_{50} : 0.7 nM, SI > 6000. In biochemical assays of RdRp compound **1** was more than 200 times more active than compound **6**.
- Topliss, J. G. *J. Med. Chem.* **1977**, 20, 463.
- Romines, K. R.; Freeman, G. A.; Schaller, L. T.; Cowan, J. R.; Gonzales, S. S.; Tidwell, J. H.; Andrews, C. W.; Stammers, D. K.; Hazen, R. J.; Ferris, R. G.; Short, S. A.; Chan, J. H.; Boone, L. R. *J. Med. Chem.* **2006**, 49, 727.
- The coordinates have been deposited to the PDB. Access code: 2RK1.
- Resistance development was performed with analog **6** in MT-2 cells, which display a slightly improved SI when compared to the MT-4 cell line. In short, HIV-1 III_B was propagated in MT-2 cells using standard procedures. In vitro selection of HIV-1 III_B with compound **6** commenced at $0.5 \times \text{EC}_{50}$ (0.4 μM). Virus was harvested when the cytopathic effect was evident in the majority of cells, marking the completion of a passage. The drug concentration was held at $0.5 \times \text{EC}_{50}$ for the first two passages, and subsequently was increased 2-fold, finally reaching 51.2 μM . Reverse transcriptase V106I was the first mutation detected, by population sequencing of a viral pool maintained at 3.2 μM ($4 \times \text{EC}_{50}$) and cultured over a total of 35 days. Clonal sequencing of the terminal passage revealed the presence of V106I (21/25 clones, 84%) and F227L (15/25 clones, 60%). Consistent with the X-ray crystallographic structural data, K103N transcriptase was also present in a minority of clones (4/25, 16%). Viral pools from passage 7 (12.8 μM) and the terminal passage (51.2 μM) both demonstrated >75-fold resistance to **6** when compared to wild-type, and 4- and 10-fold reductions in susceptibility to nevirapine, respectively. No change in susceptibility to a control compound, the NRTI tenofovir, was observed for either viral pool.